Polyaddition Enabled Functional Polymer/Inorganic Hybrid Electrolytes for Lithium Metal Batteries

Guang Yang*[abc], Yaduo Song[abc] and Longjiang Deng[abc]

a School of Electronic Science and Engineering, University of Electronic Science and Technology of China, Chengdu, 611731, China
b National Engineering Research Center of Electromagnetic Radiation Control Materials, University of Electronic Science and Technology of China, Chengdu, 611731, China
c Key Laboratory of Multi-spectral Absorbing Materials and Structures of Ministry of Education, University of Electronic Science and Technology of China, Chengdu, 611731, China

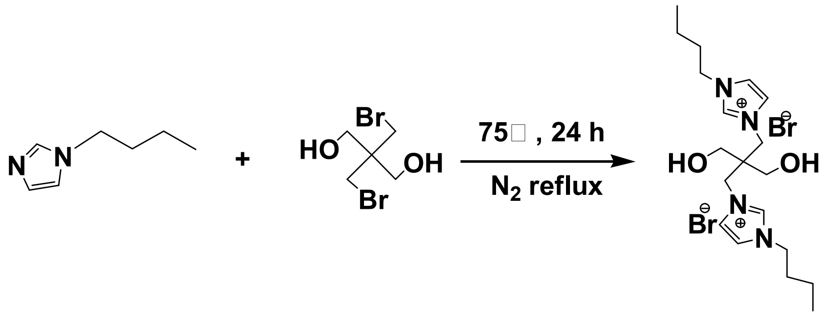

Scheme S1. Synthetic route for BBMD

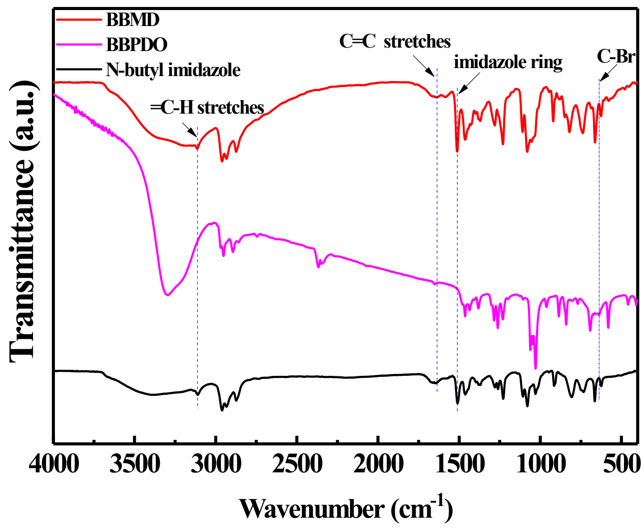

Fig. S1 FTIR spectra of BBMD, BBPDO, and N-butyl imidazole.

From FTIR curve of BBMD, the peak at 1512 cm^{-1} could be ascribed to the vibration of the imidazole ring. C-H, C=C, C=N and C-N stretching vibration on the imidazole ring appears at 3112, 1637,1581 and 1462 cm^{-1}, respectively. The peaks at 816, 736 and 661 cm^{-1} could be assigned to the out-of-plane bending vibration of the imidazole ring. The absorption peak of C-Br at 637 cm^{-1} disappeared, implying that ionic liquids have been successfully synthesized.

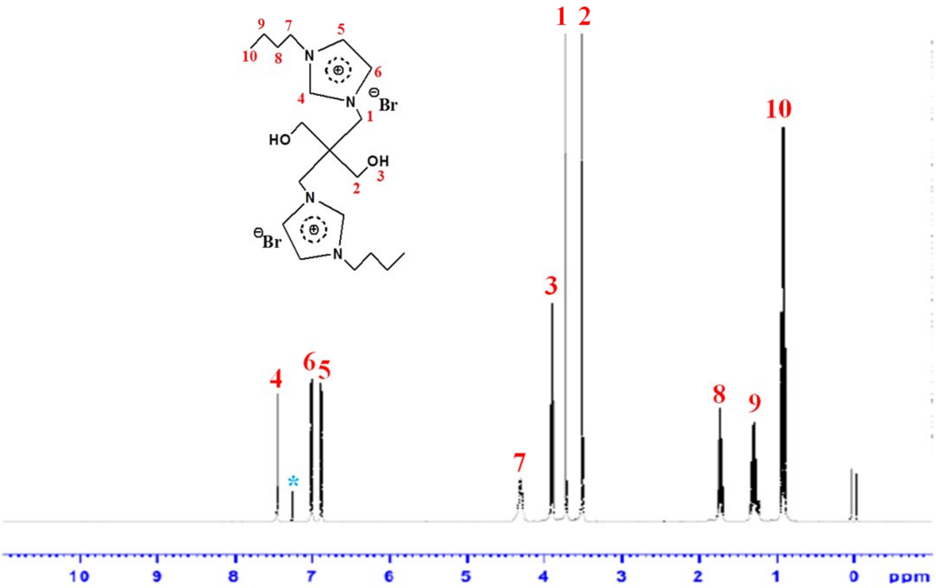

Fig.S2 ^{1}H NMR spectra of BBMD ($CDCl_3$).

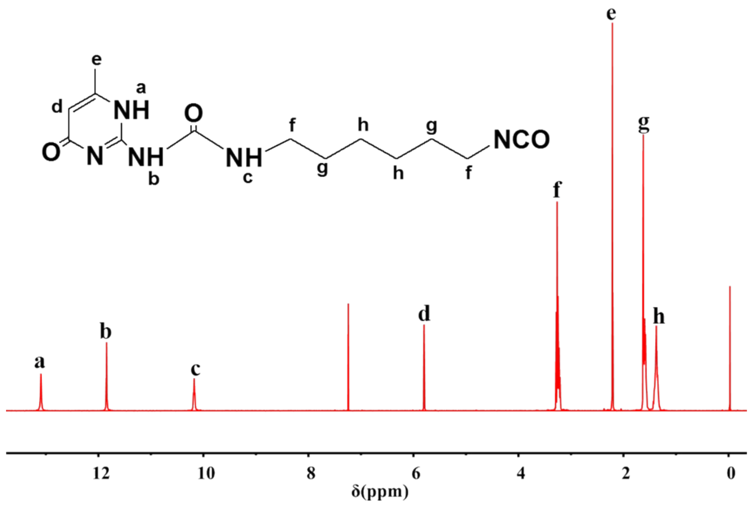

Fig.S3 ^{1}H NMR spectra of UPy-NCO ($CDCl_3$).

^1H NMR (400 MHz, 298 K, $CDCl_3$, TMS), δ: 13.09 (-N***H***-C(-NH-)=N-), 11.84 (-NH-C(-N***H***-)=N-), 10.19-10.16 (-NH-CO-N***H***-CH_2-), 5.80 (-CO-C***H***=C(CH_3)-), 3.31–3.21 (-NH-C$\underline{\boldsymbol{H}}_2$-$(CH_2)_4$-C$\underline{\boldsymbol{H}}_2$-NCO), 2.21 (-CO-CH=C(C$\underline{\boldsymbol{H}}_3$)-), 1.62–1.56 (-NH-$CH_2$-(C$\underline{\boldsymbol{H}}_2$)$_4$-$CH_2$-NCO).

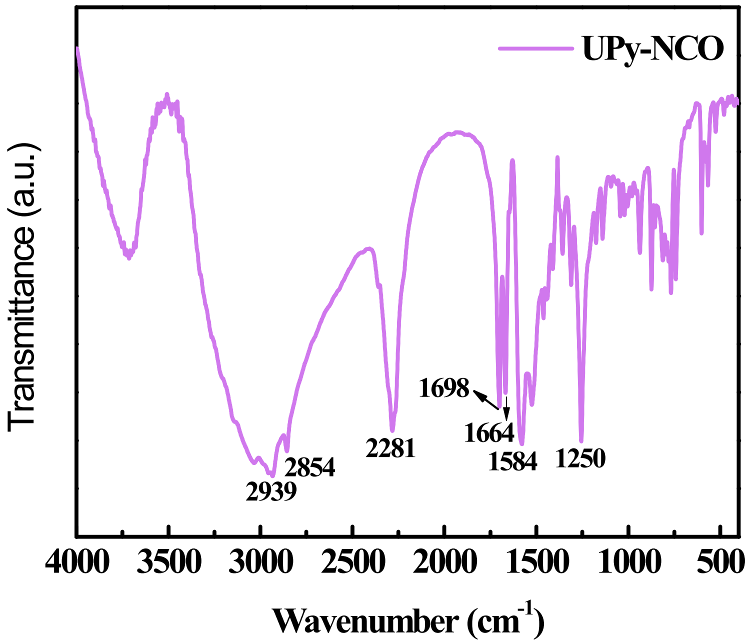

Fig.S4 FTIR spectra of UPy-NCO.

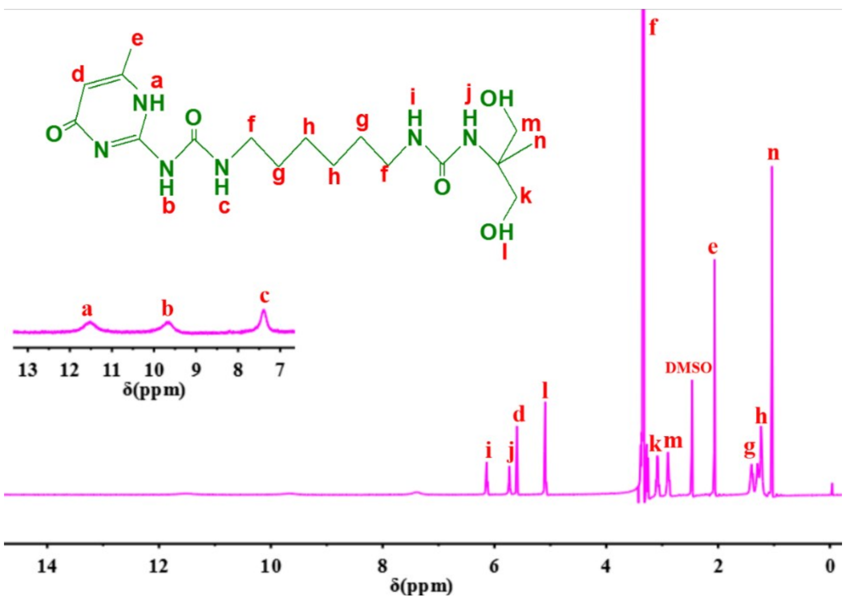

Fig.S5 ^1H NMR spectrum of UPy-diol.

^{1}H NMR (400 MHz, 298 K, DMSO, TMS), δ: 11.51 (-N***H***-C(-NH-)=N-), 9.65 (-NH-C(-N***H***-)=N-), 7.39 (-NH-CO-N***H***-CH$_2$-), 6.14 (-CH$_2$-N***H***-CO-NH-), 5.73 (-CH$_2$-NH-CO-N***H***-), 5.60 (-CO-C***H***=C-(CH$_3$)-), 5.09 (-C(CH$_2$O***H***)$_2$-CH$_3$), 3.43-3.25 (-NH-C***H***$_2$-(CH$_2$)$_4$-***CH***$_2$-NH-), 3.11-3.06 (-C(C***H***$_2$OH)$_2$-CH$_3$), 2.91-2.87 (-C(C***H***$_2$OH)$_2$-CH$_3$), 2.06 (-CO-CH=C(C***H***$_3$)-), 1.23 (-NH-CH$_2$-(C***H***$_2$)$_4$-CH$_2$-NH-), 1.04 (-C(CH$_2$OH)$_2$-C***H***$_3$).

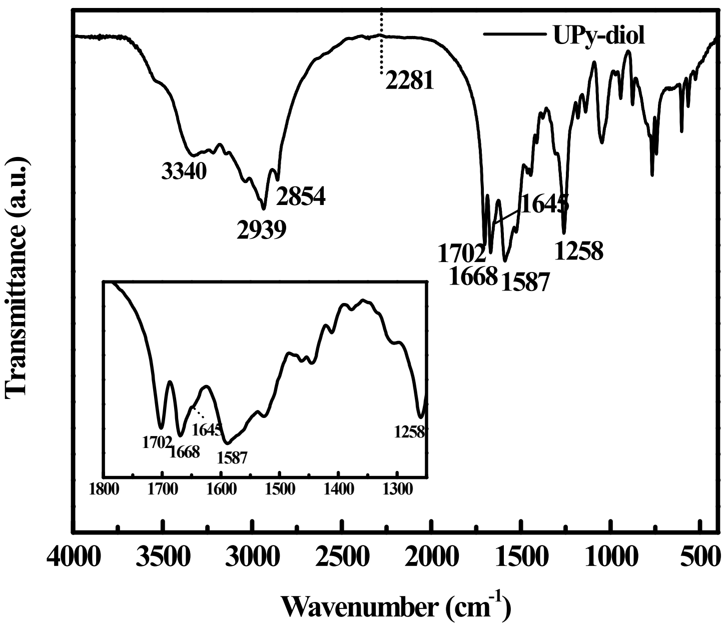

Fig.S6 FTIR spectra of UPy-diol.

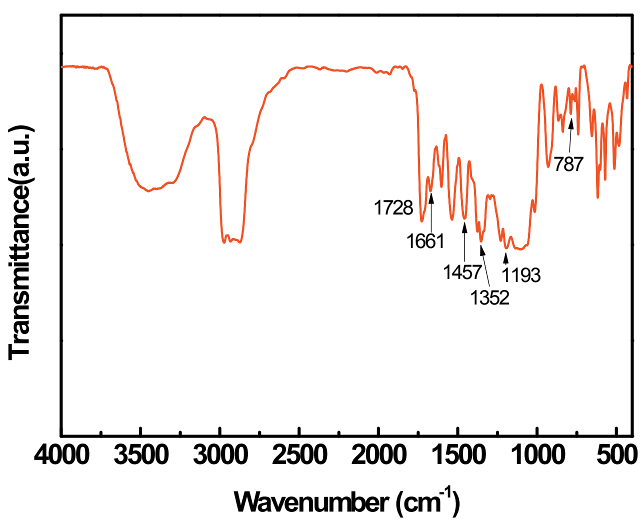

Fig.S7 FTIR spectra of $P_{0.29}I_{0.29}E_{0.29}U_{0.13}$ (10 wt.% of LiTFSI).

Fig.S8 Photo image of $P_{0.29}I_{0.29}E_{0.29}U_{0.13}$.

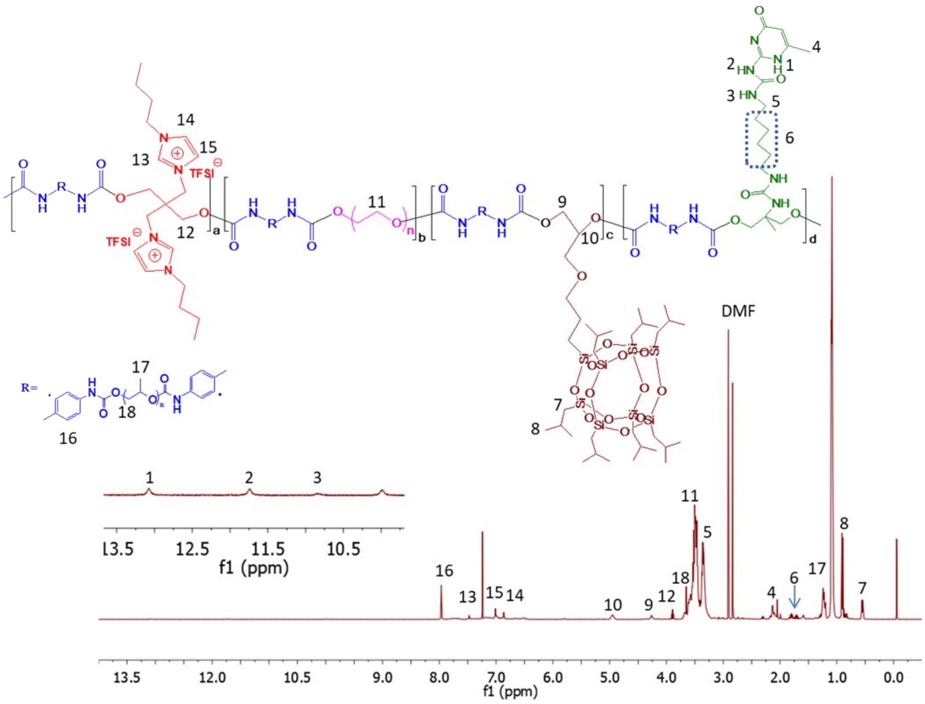

Fig.S9 ^{1}H NMR spectrum of $P_{0.29}I_{0.29}E_{0.29}U_{0.13}$ (in $CDCl_3$).

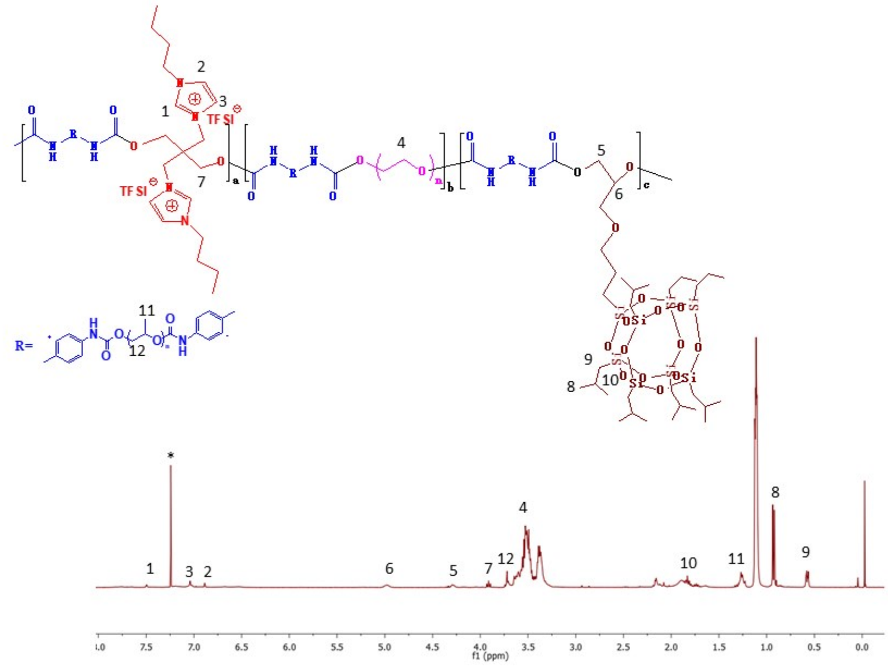

Fig.S10 ^{1}H NMR spectra of $P_{0.33}I_{0.33}E_{0.33}$ (in $CDCl_3$).

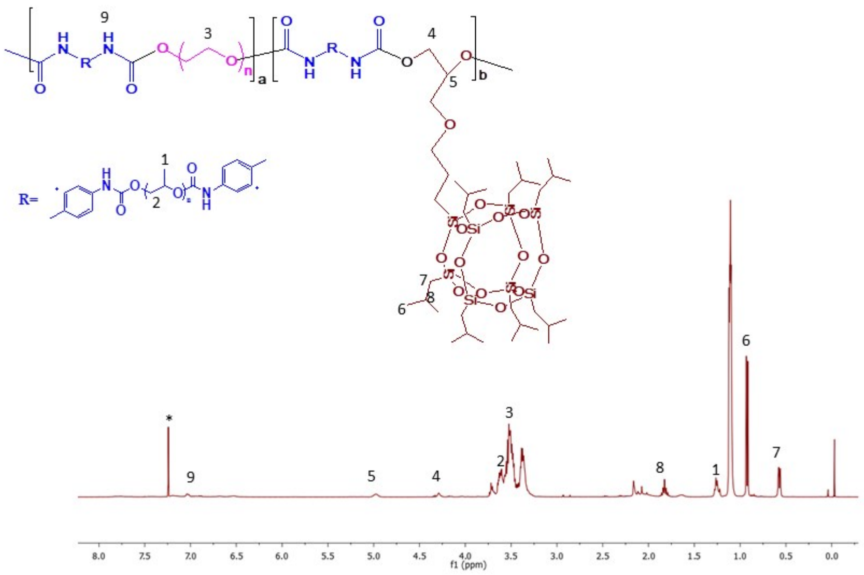

Fig.S11 ^{1}H NMR spectra of $P_{0.5}E_{0.5}$ (in $CDCl_3$).

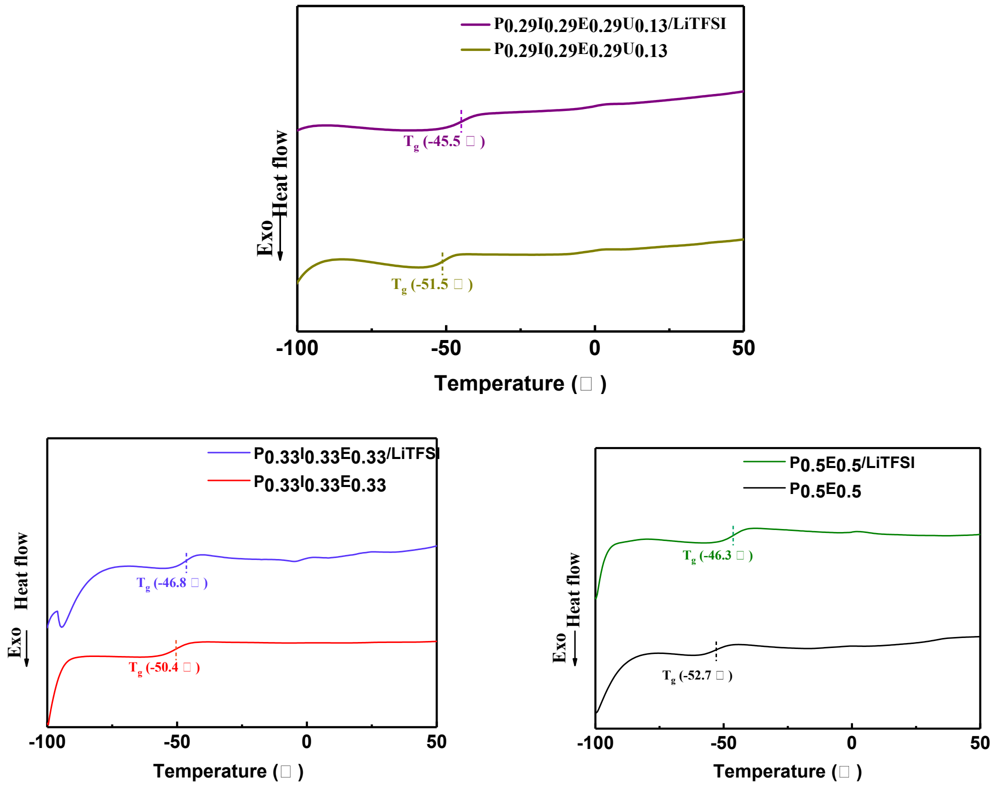

Fig.S12 DSC curves of $P_{0.29}I_{0.29}E_{0.29}U_{0.13}$, $P_{0.33}I_{0.33}E_{0.33,}$ and $P_{0.5}E_{0.5}$ with and without 10 wt.% of LiTFSI.

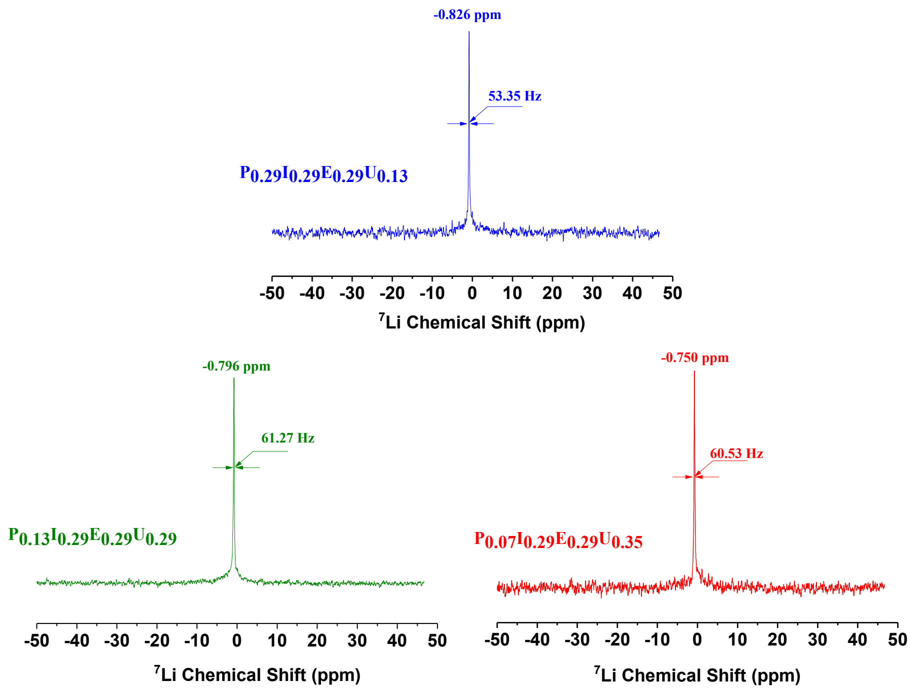

Fig.S13 ^{7}Li ssNMR spectra of $P_{0.29}I_{0.29}E_{0.29}U_{0.13}$, $P_{0.13}I_{0.29}E_{0.29}U_{0.29}$, and $P_{0.07}I_{0.29}E_{0.29}U_{0.35}$ (10 wt.% of LiTFSI).

$$\sigma(T)=\frac{A}{\sqrt{T}}\exp\left(\frac{-B}{R(T-T_0)}\right)$$

Equation S1

Table S1. Summary of chemical shift and line width from Fig.S13.

Sample	**^{7}Li chemical shift (ppm)**	**NMR line width (Hz)**
$P_{0.29}I_{0.29}E_{0.29}U_{0.13}$	-0.826	53.34857
$P_{0.13}I_{0.29}E_{0.29}U_{0.29}$	-0.796	61.26651
$P_{0.07}I_{0.29}E_{0.29}U_{0.35}$	-0.750	60.53322

Table S2. Summary of Raman shift and relative fraction Fig.4.

Sample	v-C_{free}	fraction-C_{free}	v-C_{coord}	fraction-C_{coord}
$P_{0.5}E_{0.5}$	737.4	44.9	744.5	55.1
$P_{0.33}I_{0.33}E_{0.33}$	737.8	52.5	744.6	47.5
$P_{0.29}I_{0.29}E_{0.29}U_{0.13}$	738.7	65.2	745.2	34.8

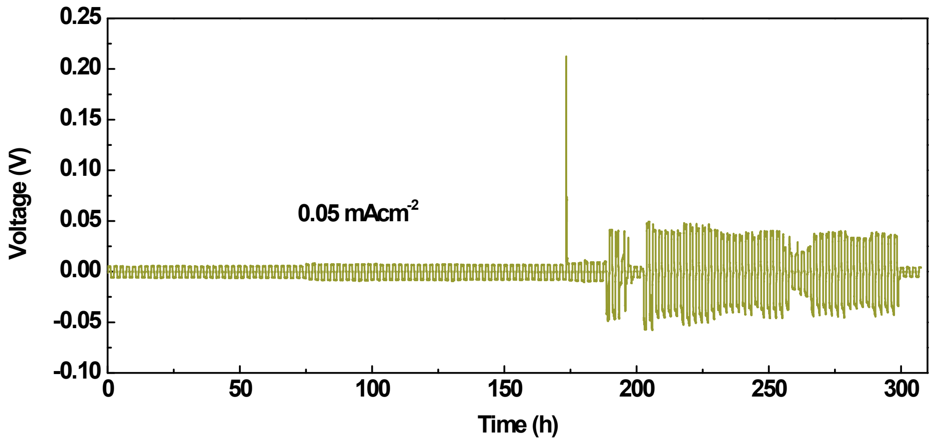

Fig.S14 Stripping/plating cycles of Li/Li symmetrical cells with electrolyte containing 1 M LiTFSI in EC/DMC (1:1, v/v) at a current density of 0.05 mA/cm^2.

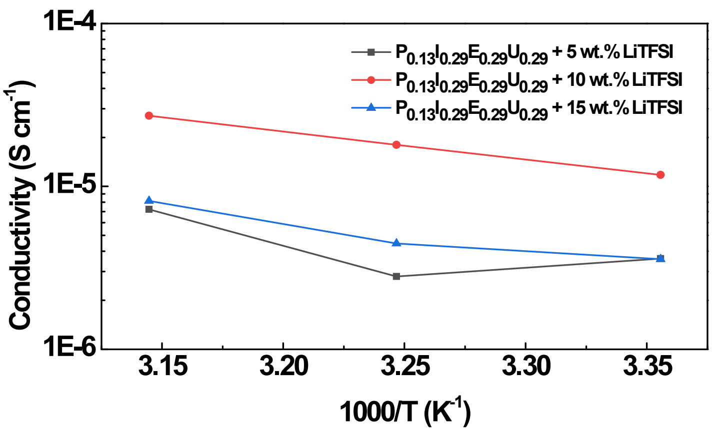

Fig.S15 Conductivity profile of $P_{0.13}I_{0.29}E_{0.29}U_{0.29}$ as a function of LiTFSI weight percentage.

The ion conductivities of $P_{0.13}I_{0.29}E_{0.29}U_{0.29}$ (randomly chosen) doped with different mass fractions of LiTFSI (5 wt%,10wt%,15wt %) were measured and it was found that the ion conductivity of $P_{0.13}I_{0.29}E_{0.29}U_{0.29}$ doped with10 wt.% LiTFSI was the highest. In the main text, we kept 10 wt.% of LiTFSI in the samples for measurement.

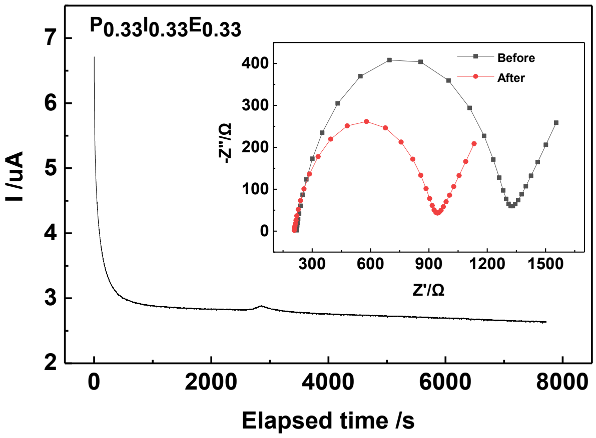

Fig.S16 Chronoamperometry curves of Li/$P_{0.33}I_{0.33}E_{0.33}$/Li cell with inset EIS profiles before and after polarization. (60 ℃).

The t_{Li+} was calculated to be 0.14 for $P_{0.33}I_{0.33}E_{0.33}$.

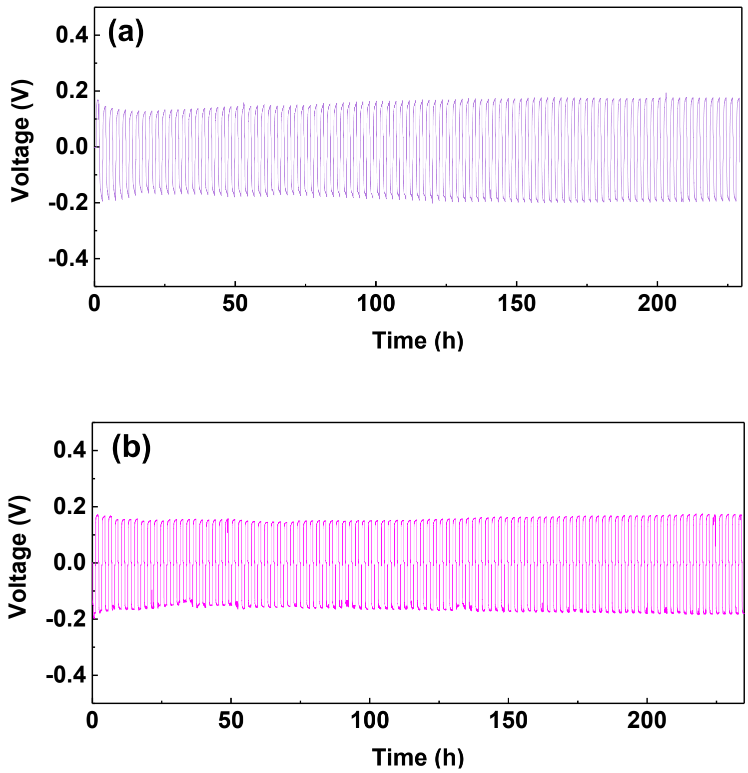

Fig.S17 Stripping/plating cycles of Li/Li symmetrical cells with $P_{0.5}E_{0.5}$ (a) and $P_{0.33}I_{0.33}E_{0.33}$(b) at a current density of 0.05 mA/cm^2 (60 ℃).

The overpotential of Li/Li symmetrical cells with $P_{0.5}E_{0.5}$ is ~0.18 V and the overpotential of Li/Li symmetrical cells with $P_{0.33}I_{0.33}E_{0.33}$ is ~0.16 V. Both were higher than Li/$P_{0.29}I_{0.29}E_{0.29}U_{0.13}$/Li cell in the main text.

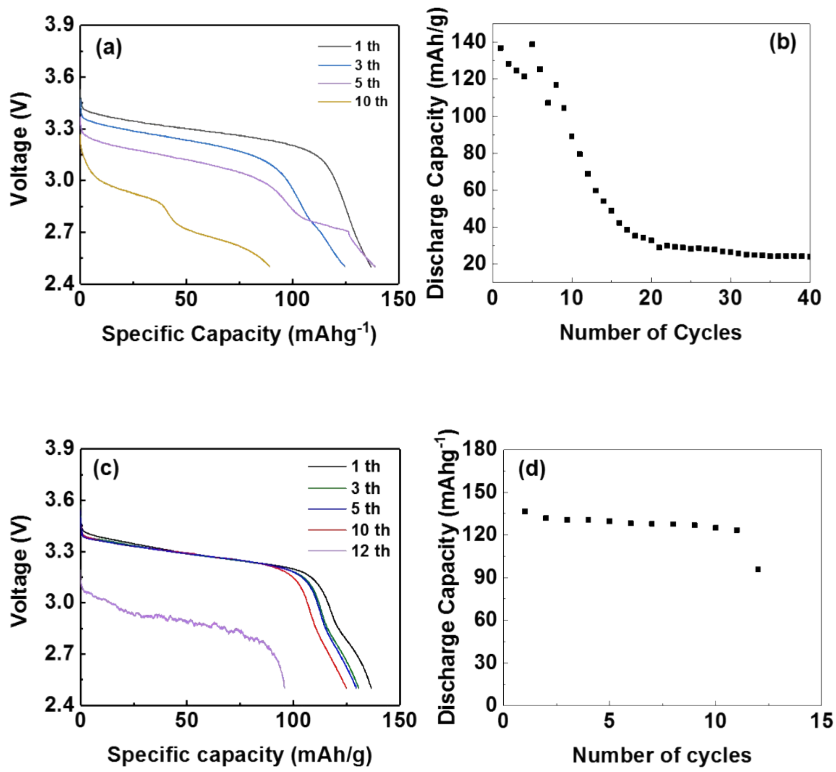

Fig.S18 Discharge curves of Li/ LFP cell with $P_{0.5}E_{0.5}$ (a) and $P_{0.33}I_{0.33}E_{0.33}$ (c) at 0.1 C; Cycling performance of Li/ LFP cell with $P_{0.5}E_{0.5}$ (b) and $P_{0.33}I_{0.33}E_{0.33}$ (d) at 0.1 C. (60 ℃)